THE JOURNAL OF BIOLOGICAL CHEMISTRY VOL. 288, NO. 1, pp. 264–273, January 4, 2013

Filamin Interacts with Epithelial Sodium Channel and Inhibits Its Channel Function*

Received for publication, June 29, 2012, and in revised form, November 9, 2012 Published, JBC Papers in Press, November 16, 2012, DOI 10.1074/jbc.M112.396408

Qian Wang[1], **Xiao-Qing Dai, Qiang Li, Jagdeep Tuli, Gengqing Liang, Shayla S. Li, and Xing-Zhen Chen**[2]

From the Membrane Protein Disease Research Group, Department of Physiology, Faculty of Medicine and Dentistry, University of Alberta, Edmonton, Alberta, T6G 2H7, Canada

Background: ENaC is critical in Na^+ homeostasis and blood pressure, but how it is regulated by the cytoskeleton remains unclear.
Results: Filamins, important actin filament components, interact with ENaC and inhibit its channel function.
Conclusion: Filamins interact with surface ENaC for structural purposes and for regulating its channel function.
Significance: The ENaC-filamin interaction may be important in the pathogenesis associated with altered ENaC function.

Epithelial sodium channel (ENaC) in the kidneys is critical for Na^+ balance, extracellular volume, and blood pressure. Altered ENaC function is associated with respiratory disorders, pseudohypoaldosteronism type 1, and Liddle syndrome. ENaC is known to interact with components of the cytoskeleton, but the functional roles remain largely unclear. Here, we examined the interaction between ENaC and filamins, important actin filament components. We first discovered by yeast two-hybrid screening that the C termini of ENaC α and β subunits bind filamin A, B, and C, and we then confirmed the binding by *in vitro* biochemical assays. We demonstrated by co-immunoprecipitation that ENaC, either overexpressed in HEK, HeLa, and melanoma A7 cells or natively expressed in LLC-PK1 and IMCD cells, is in the same complex with native filamin. Furthermore, the biotinylation and co-immunoprecipitation combined assays showed the ENaC-filamin interaction on the cell surface. Using *Xenopus* oocyte expression and two-electrode voltage clamp electrophysiology, we found that co-expression of an ENaC-binding domain of filamin substantially reduces ENaC channel function. Western blot and immunohistochemistry experiments revealed that the filamin A C terminus (FLNAC) modestly reduces the expression of the ENaC α subunit in oocytes and A7 cells. After normalizing the current by plasma membrane expression, we found that FLNAC results in ~50% reduction in the ENaC channel activity. The inhibitory effect of FLNAC was confirmed by lipid bilayer electrophysiology experiments using purified ENaC and FLNAC proteins, which showed that FLNAC substantially reduces ENaC single channel open probability. Taken together, our study demonstrated that filamin reduces ENaC channel function through direct interaction on the cell surface.

The epithelial sodium channel (ENaC)[3]/degenerin family represents a class of ion channels discovered in the early 1990s (1). Members of this family are involved in Na^+ and H_2O reabsorption, taste, touch, and acid-base homeostasis and are divided into four main subfamilies as follows: ENaC; FMRF (Phe-Met-Arg-Phe)-amide-gated channels; acid-sensing ion channels, and mechanosensory channel proteins of nematode degenerins. This family includes more than 20 members that all possess two transmembrane domains plus intracellular N and C termini and are Na^+-selective and amiloride-inhibitable (2–5).

ENaC has small conductance (~5 picosiemens) and is putatively composed of two α subunits (α-ENaC, 669 aa), one regulatory β subunit (β-ENaC, 640 aa), and one regulatory γ subunit (γ-ENaC, 649 aa) ($2\alpha1\beta1\gamma$) arranged pseudosymmetrically around the channel pore. It is known that actin filament is an important regulator of the ENaC channel and that ENaC directly binds α-spectrin, ankyrin, and F-actin (6, 7). ENaC is sensitive to membrane stretch, hydrostatic pressure, and shear stress, as showed in *Xenopus* oocytes, mammalian cultured cells, artificial lipid bilayers, and native tissues (8, 9). In the kidneys, ENaC plays a critical role in Na^+ balance, extracellular volume, and blood pressure. In the lungs, ENaC has a distinct role in controlling the ionic content of the air-liquid interface thereby determining the rate of mucociliary transport. In human and animal models, abnormal ENaC activity leads to a number of pathologies, *e.g.* hypertension, altered mucociliary transport, respiratory distress, and high altitude pulmonary edema. Loss-of-function mutations in ENaC cause salt-wasting syndrome in pseudohypoaldosteronism type 1, whereas gain-of-function mutations in β- and γ-ENaC cause Liddle syndrome, a form of salt-sensitive hypertension (2, 3, 10–12).

Filamins are large cytoplasmic proteins that cross-link cortical actin into a dynamic three-dimensional structure and were discovered as the first family of nonmuscle actin-binding proteins. Mammalian filamins consist of three actin-binding homologs (A, B, and C), each of ~280 kDa and containing an N-terminal actin-binding domain (~300 aa), followed by a long rod-like domain made of 24 repeats of anti-parallel β-sheets

* This work was supported in part by the Canadian Institutes of Health Research and the Kidney Foundation of Canada (to X. Z. C.).
[1] Recipient of a studentship from the Natural Sciences and Engineering Research Council of Canada (NSERC), Collaborative Research and Training Experience.
[2] Senior Scholar of the Alberta Innovates, Health Solutions. To whom correspondence should be addressed. Tel.: 780-492-2294; Fax: 780-492-8915; E-mail: xzchen@ualberta.ca.
[3] The abbreviations used are: ENaC, epithelial sodium channel; FLNAC, filamin A C terminus; aa, amino acid; IB, immunoblot; WB, Western blot; FLNA, filamin A; FLNB, filamin B; IMCD, inner medullary collecting duct; MDCK, Madin-Darby canine kidney; NMDG, *N*-methyl-D-glucamine; IP, immunoprecipitation; IHC, immunohistochemistry.

(~96 aa each) and two "hinge" regions. Two filamin molecules self-associate to form a homodimer through the last C-terminal repeat, which allows the formation of a V-shaped flexible structure that is essential for the function (13, 14). Current data suggest that filamins are involved in the organization of the cytoskeleton, which is important for cell adhesion and motility, and interact with and regulate several membrane proteins (ion channels, receptors, β-integrins, and glycoprotein Ibα) and cytoplasmic signaling proteins (Rho GTPases, TRAF2, Smads, and SEK-1) (13–20). Nevertheless, a clear mechanistic explanation for their importance is still lacking. Genetic evidence indicates that filamins are essential for human development, and mutations in either filamin A (FLNA) or -B (FLNB) have been associated with abnormal development of brain, bone, cardiovascular system, and several other organs. Although different filamin isoforms seem to have distinct roles in development, they may also be functionally similar and confer genetic redundancies that lead, upon mutations, to a wide degree of variances in the genetic syndromes.

The C terminus of α-ENaC has been shown to be important for channel modulation by the actin cytoskeleton (21). However, whether and how actin-binding proteins influence the function of ENaC remain poorly understood. In this study, we employed various approaches of molecular biology and electrophysiology to investigate physical and functional interactions between ENaC and filamins, with an emphasis on using the pore-forming α-ENaC and the predominant filamin A isoform.

EXPERIMENTAL PROCEDURES

Antibodies—Four rabbit polyclonal α-ENaC antibodies, anti-α-ENaC 324870 (Calbiochem), anti-α-ENaC ENACA11-A (Alpha Diagnostic Inc., San Antonio, TX), anti-α-ENaC PA1–920A (Pierce), and anti-α-ENaC C-20 (Santa Cruz Biotechnology, Santa Cruz, CA), were used in this study. Anti-β-ENaC H-190 and anti-γ-ENaC F-20 were purchased from Santa Cruz Biotechnology. Anti-FLNA antibodies were mouse monoclonal FIL2 antibodies raised using the filamin antigen purified from chicken gizzard (Sigma), mouse monoclonal anti-FLNA E-3, and rabbit polyclonal anti-FLNA H-300 (Santa Cruz Biotechnology). Anti-GST B-14 (Santa Cruz Biotechnology) and anti-His 27E8 (Cell Signaling, Danvers, MA) antibodies were used in the GST pulldown assay. Mouse anti-GFP B-2 (Santa Cruz Biotechnology) was used in immunoblotting (IB) of GFP-tagged proteins. Anti-β-actin antibody C-4 (Santa Cruz Biotechnology) was used in Western blot (WB) for loading controls.

Human Melanoma Cell Lines—Human melanoma M2 cells are deficient in FLNA. Transfection of FLNA into M2 cells generated A7 cells. To generate M2 and A7 ENaC stable cell lines, 600 mg/ml hygromycin and G418 (Invitrogen) were added to select viable clones one recovery day following transfection and then maintained using hygromycin (100 μg/ml) (M2) or hygromycin plus G418 (300 μg/ml) (A7).

Cell Culture and Transfection—Human embryonic kidney (HEK293), HeLa, mouse inner medullary collecting duct (IMCD), Madin-Darby canine kidney (MDCK), porcine kidney cells LLC-PK1, and M2 and A7 cells were cultured in Dulbecco's modified Eagle's medium (DMEM) supplemented with L-glutamine, penicillin/streptomycin, and 10% fetal bovine serum (FBS). Transfection of ENaC was performed on HEK293, HeLa, and MDCK cells cultured to 90% confluency using Lipofectamine 2000 (Invitrogen) according to the manufacturer's protocol.

Plasmid Construction—The C termini of human filamin A (NM_001456, FLNAC, aa 2150–2647) and filamin B (NM_001457, FLNBC, aa 2105–2602) were isolated from either the human kidney cDNA library or HEK293 cells. The C terminus of filamin C (NM_001458, FLNCC, aa 2144–2725) was cut from pACT2-FLNCC plasmid. cDNAs were subcloned into pGADT7 (Clontech) for yeast expression, pET28a (Novagen, EMD Chemicals, Gibbstown, NJ) for bacterial expression, pcDNA3.1 for mammalian expression, and pCHGF for *Xenopus* oocyte expression. Human α-ENaC N terminus (α-ENaCN, aa 1–82), α-ENaC C terminus (α-ENaCC, aa 588–669), β-ENaC N terminus (β-ENaCN, aa 1–14), β-ENaC C terminus (β-ENaCC, aa 559–640), γ-ENaC N terminus (γ-ENaCN, aa 1–76), and γ-ENaC C terminus (γ-ENaCC, aa 568–649) were subcloned into pGBKT7 (Clontech) for yeast expression. α-ENaCC and β-ENaCC were constructed into vector pGEX5X (Pharmacia, Piscataway, NJ) for GST pulldown assay. Human α-ENaC and β-ENaC were subcloned into vectors pcDNA3.1 and pEGFPC2, in which GFP was fused to the N terminus for mammalian expression. Rabbit α, β, and γ subunits of ENaC in pSD series vector for oocyte expression were the generous gifts of Dr. L. Schild from the University of Lausanne. All plasmid constructions have been confirmed by sequencing.

Yeast Two-hybrid Analysis—A yeast two-hybrid screen was performed in the yeast strain AH109 containing *Ade2*, *His3,* and *lacZ* reporter genes under the control of the GAL4 upstream-activating sequences as described before (22). Briefly, the cDNAs encoding ENaC fragments were subcloned in-frame into the GAL4 DNA-binding domain of vector pGBKT7 by a PCR-based approach. Both C and N termini of ENaC subunits were used as baits to screen human kidney and heart cDNA libraries (Clontech) constructed in vector pGADT7 containing the GAL4 activation domain. Transformants were grown on the minimal synthetic dropout medium lacking leucine, tryptophan, adenine, and histidine. Colonies survived were further screened for activation of a *lacZ* reporter gene by a filter lift assay (Clontech). Plasmid cDNAs were isolated from the positive colonies and individually tested against the bait and empty vector.

GST Pulldown—Pre-cleared bacterial protein extracts (250 μl) containing GST-α-ENaCC, GST-β-ENaCC, or GST alone were incubated with 2 μg of purified His-FLNAC in the binding buffer (50 mM Tris, pH 7.5, 150 mM NaCl, 1 mM $CaCl_2$). The mixture was incubated at room temperature (RT) for 1 h with gentle shaking, followed by another hour of incubation after addition of 100 μl of glutathione-agarose beads (Sigma). The beads were then washed 4–5 times with 140 mM NaCl, 10 mM Na_2HPO_4, 1.8 mM KH_2PO_4, pH 7.5, and the remaining proteins were eluted using 10 mM glutathione, 50 mM Tris, pH 8.0. The protein samples were then prepared for WB.

Co-immunoprecipitation (Co-IP)—Co-IP was performed using lysate of native IMCD and LLC-PK1, ENaC-transfected HEK293 and HeLa cells, and α-ENaC stably expressed A7 cell

line. A cell monolayer in 100-mm dishes was washed twice with phosphate-buffered saline (PBS) and solubilized in ice-cold CellLytic-M lysis buffer and proteinase inhibitor mixture (Sigma). Supernatant was collected following centrifugation at 16,000 × *g* for 15 min. Equal amounts of total protein from postnuclear supernatants were pre-cleared for 1 h with protein G-Sepharose (GE Healthcare) and then incubated for 4 h in a cold room with antibody against ENaC or FLNA. After the addition of 100 μl of 50% protein G-Sepharose, the mixtures were incubated overnight with gentle shaking. The immune complexes absorbed to protein G-Sepharose were washed five times with the Nonidet P-40 lysis buffer (50 mM Tris, pH 7.5, 150 mM NaCl, 1% Nonidet P-40) with proteinase inhibitor. The precipitated proteins were analyzed by WB using antibodies against FLNA or ENaC.

Preparation of mRNAs and Microinjection into Oocytes—Capped synthetic rabbit α, β, and γ subunits of ENaC mRNAs were synthesized by *in vitro* transcription from a linearized template in the pSD series vector using the mMESSAGE mMACHINE1 kit (Ambion, Austin, TX). FLNAC and FLNBC in the pCHGF vector were used to synthesize their mRNAs in a similar way. α- and γ-ENaC were linearized by PvuII and β-ENaC by BgIII; FLNAC and FLNBC were linearized by MluI. Stage V–VI oocytes were prepared as previously described (23). Each oocyte was injected with 50 nl of water containing mRNA of ENaC subunits (10 ng each) alone or together with 20 ng of FLNAC mRNA 5 h following defolliculation. An equal volume of RNase-free water was injected into each control oocyte. Injected oocytes were incubated at 16–18 °C in the Barth solution supplemented with penicillin/streptomycin and 2 μM amiloride for 2–3 days (to reduce Na^+ loading via ENaC) prior to experiments.

Two-electrode Voltage Clamp—Two-electrode voltage clamp was performed as described previously (23). Briefly, the two electrodes (capillary pipettes, Warner Instruments, Hamden, CT) impaling *Xenopus* oocytes were filled with 3 M KCl to form a tip resistance of 0.3–2 megohms. Oocyte whole-cell currents were recorded using a Geneclamp 500B amplifier and Digidata 1322A AD/DA converter (Molecular Devices, Union City, CA). Gap-free and voltage ramp protocols, as described previously (24), were used in experiments, with current/voltage signals sampled at intervals of 100 ms and 100 μs, respectively. The standard sodium solution contained 100 mM NaCl, 2 mM KCl, 1 mM $CaCl_2$, 1 mM $MgCl_2$, 10 mM HEPES, and pH 7.5. *N*-Methyl-D-glucamine (NMDG, Acros Organics, Monroeville, NJ) was used to replace Na^+ to generate the NMDG-containing solution.

Protein Preparation and Lipid Bilayer Electrophysiology—Human α-, β-, and γ-ENaC proteins were purified from MDCK cell lines stably transfected with pGTAP3F-ENaC subunits. TAP-ENaC was prepared and reconstituted in a lipid bilayer system as described previously (25) to assess the channel activity. Briefly, PC-ONE amplifier (Dagan Corp., Minneapolis, MN) in combination with Clampex 9 program (Molecular Devices) was used in these experiments. The *cis* (or *trans*) compartment contained 150 (or 15) mM NaCl, 15 μM Ca^{2+}, pH 7.4 (adjusted by MOPS-KOH). TAP-α-ENaC protein was added to the *cis* chamber in proximity of the membrane or used to directly "paint" the membrane. To examine the effect of *Escherichia coli* purified FLNAC on α-ENaC, single channel activity of α-ENaC was recorded for 20–40 min before and after the addition of FLNAC.

Biotinylation—*Xenopus* oocytes and HeLa or M2 cells were washed three times with Barth solution/PBS before incubation with 5 or 1 mg/ml Sulfo-NHS-SS-Biotin (Pierce) for 30 min at RT. After adding 1 M NH_4Cl to quench the nonreacted biotinylation reagent, oocytes/cells were washed with Barth solution/PBS and then harvested in ice-cold CellLytic-M lysis buffer and proteinase inhibitor mixture. Oocyte/cell lysates were incubated at RT for 3 h with gentle shaking upon addition of 100 μl of streptavidin (Pierce). The surface protein absorbed by streptavidin was resuspended in SDS and subjected to SDS-PAGE.

Immunohistochemistry—Immunohistochemistry was used to determine the surface expression of ENaC with or without FLNAC co-expression in *Xenopus* oocytes. Oocytes were washed with PBS and then fixed in 3% paraformaldehyde for 15 min at RT. After washing three times with 50 mM NH_4Cl in PBS, oocytes were permeabilized with 0.1% Triton X-100 for 4 min. After rinsing in PBS, oocytes were blocked in 2% bovine serum albumin for 30 min before incubating with anti-α-ENaC PA1–920A (1:100) in blocking buffer for 1 h at RT. Oocytes were then washed three times with PBS and incubated with a secondary FITC-conjugated anti-rabbit antibody (1:200) for 30 min at RT. After washing, oocytes were mounted in VECTASHIELD (Vector Laboratories, Burlingame, CA) on slides with secure-seal spacers (Grace Bio-Labs, Inc., Bend, OR) for fluorescence detection with a Zeiss 510 confocal laser-scanning microscope. Signals were quantified by ImageJ (National Institutes of Health, Bethesda).

Data Analysis and Statistics—Data were analyzed and plotted by Sigmaplot 11 or 12, and expressed as means ± S.E. (*n*), where *n* indicates the number of independent measurements. Comparisons between two sets of data were analyzed by *t* test. A probability value (*p*) of less than 0.05 and 0.01 was considered significant and very significant, respectively.

RESULTS

Physical Interaction between ENaC and Filamins—We employed a yeast two-hybrid system to screen proteins that associate with the C terminus of human α-ENaC (α-ENaCC, aa 588–669). α-ENaCC was constructed into the pGBKT7 vector, as bait, to screen human kidney and heart cDNA libraries. We found that the C terminus of human filamin A (FLNAC, aa 2150–2647) from the heart library binds α-ENaCC. We then performed one-to-one yeast two-hybrid assays and found that the C termini of three human filamins (FLNAC, aa 2150–2647; FLNBC, aa 2105–2602; FLNCC, aa 2144–2725) bind α-ENaCC and the C terminus of human β-ENaC (β-ENaCC, aa 559–640) (Fig. 1*A*), despite the fact that there is no significant sequence similarity among the C termini of α and β subunits of ENaC. To confirm the results obtained from our yeast two-hybrid experiments, we performed *in vitro* GST fusion protein affinity binding assays. For this, α- and β-ENaCC were constructed in the pGEX-5X vector in-frame with a GST epitope and expressed in the bacterial strain BL21 under the induction of 1 mM isopropyl

A

bait (PGBKT7) \ prey (PGADT7)	FLNAC (2150-2647)	FLNBC (2105-2602)	FLNCC (2144-2725)	Vector (Control)
α-ENaCN (1-82)	-	-	-	-
α-ENaCC (588-669)	++	++	++	-
β-ENaCN (1-47)	-	-	-	-
β-ENaCC (559-640)	++	++	++	-
γ-ENaCN (1-76)	-	-	-	-
γ-ENaCC (568-649)	Self-activation, not tested for binding			
Vector (Control)	-	-	-	-

B

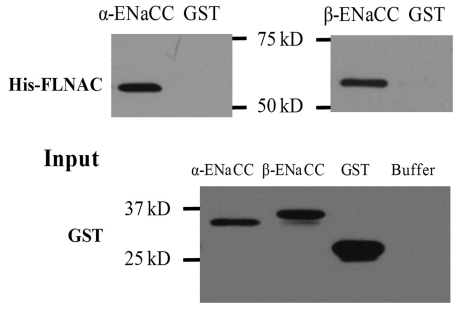

FIGURE 1. **Physical interaction between ENaC and filamins.** *A,* yeast two-hybrid assays for the ENaC-filamin interaction. ++ and − indicate the presence of a strong interaction and the absence of the interaction, respectively. *B,* interaction between ENaC and FLNA C termini by *in vitro* GST pulldown assays. Shown are representative data from three independent experiments using *E. coli* lysates containing GST-α-ENaCC, GST-β-ENaCC, or GST alone to incubate with purified His-FLNAC on the membrane. The expression of GST-tagged α-/β-ENaCC and GST is shown as *Input* (*lower panel*) by IB with GST B-14 antibody. Buffer served as a nonprotein control.

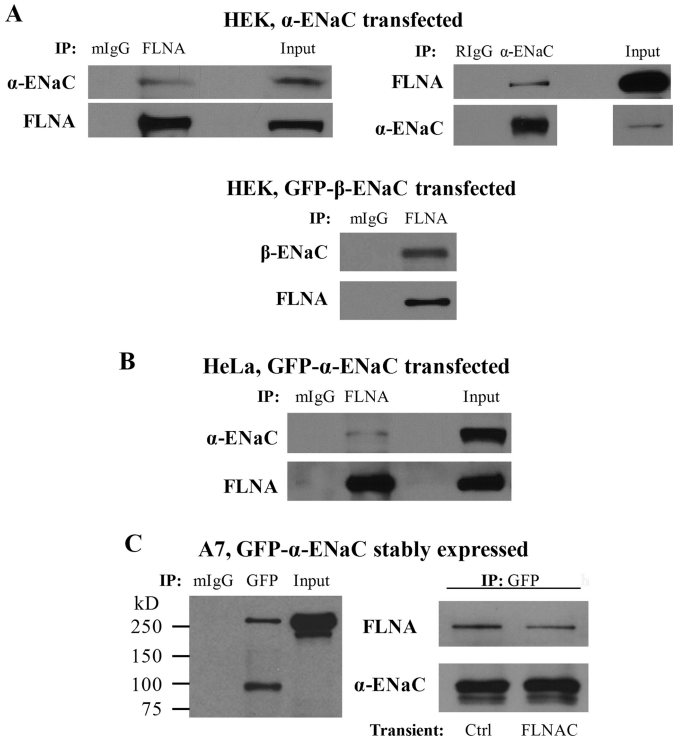

FIGURE 2. **Interaction between ENaC and filamin A by co-IP.** Data shown here are representative of those from three to five independent experiments. *A, upper panels*, HEK293 cells overexpressing α-ENaC. Cell lysates were used for reciprocal co-IP assays, using anti-FLNA E-3 or anti-α-ENaC (Calbiochem) antibody for IP or IB, as indicated. Nonimmune serum mouse IgG (*mIgG*) and rabbit IgG (*RIgG*) were used as controls. *Lower panels*, cell lysates from HEK293 cells overexpressing GFP-β-ENaC were precipitated with anti-FLNA E-3 or mouse IgG (control). Immunoprecipitated proteins were analyzed by WB using anti-FLNA E-3 or anti-GFP (Santa Cruz Biotechnology) antibody. *B,* lysates from HeLa cells overexpressing GFP-α-ENaC were precipitated with anti-FLNA E-3 or mouse IgG (control). Immunoprecipitated proteins were analyzed by WB using anti-FLNA E-3 or anti-GFP. *C,* A7 cells stably expressing GFP-α-ENaC were used for IP using GFP or mouse IgG (control). Immunoprecipitated proteins were detected with anti-FLNA E-3 or anti-GFP (*left panels*). *Right panels*, A7 cells stably expressing GFP-α-ENaC were transiently transfected with empty vector (*Ctrl*) or the FLNAC fragment. GFP antibody was used for IP, and anti-FLNA E-3 and anti-GFP were used for IB.

1-thio-β-D-galactopyranoside, and then cell lysate was collected (Fig. 1*B*). His-tagged FLNAC was similarly expressed and purified. Both α- and β-ENaCC overexpressed in *E. coli* were able to interact with purified FLNAC (Fig. 1*B*).

To determine whether ENaC subunits bind FLNA *in vivo*, we overexpressed α-ENaC and β-ENaC in the HEK293 cell line and performed co-IP. Both α-ENaC and β-ENaC were found to interact with native FLNA (Fig. 2*A*). In HeLa cells transfected with GFP-α-ENaC, anti-FLNA E-3 antibody was able to precipitate GFP-α-ENaC (Fig. 2*B*), indicating that the two proteins are in the same complex. Moreover, in the A7 α-ENaC stably expressing cell line, FLNA was found to interact with GFP-α-ENaC (Fig. 2*C*). Furthermore, the presence of FLNAC through overexpression reduced the interaction of α-ENaC with full-length FLNA (Fig. 2*C*), presumably through competitive binding.

The endogenous ENaC-FLNA interaction was confirmed using native IMCD and LLC-PK1 cell lines. FLNA protein was detected in the precipitates of LLC-PK1 and IMCD cells using an anti-α-ENaC antibody but not in the precipitates using nonimmune IgG (Fig. 3, *A* and *B*). Reciprocally, α-ENaC signal was observed in the precipitates of LLC-PK1 using an antibody against FLNA for IP. These data demonstrated that α-ENaC and FLNA are in the same complex *in vivo*. Thus, ENaC interacts with filamins *in vitro* and *in vivo*.

Because ENaC channels mainly exhibit their channel function on the plasma membrane, we wondered whether surface ENaC interacts with filamins. For this we first isolated surface membrane proteins by biotinylation assays using HeLa cells with or without overexpression of HA-tagged α-ENaC. Both streptavidin-absorbed and flow-through lysates were immunoblotted with antibody against α-ENaC, FLNA, or Na/K-ATPase. We found that overexpression of ENaC results in increased biotinylated ENaC and FLNA but not Na/K-ATPase (Fig. 3*C*), suggesting that more FLNA molecules are specifically recruited to complex with an increased population of the surface membrane ENaC. We then performed co-IP assays using biotinylated lysates to directly examine their interaction on the surface membrane. For this purpose we utilized the monomeric avidin kit (Pierce) that allows biotinylated lysates to dissociate from streptavidin without disrupting protein complexing in the lysates. Indeed, our experiments using HeLa and M2 cells demonstrated that ENaC channels located on the plasma membrane interact with FLNA (Fig. 3*D*).

Of note, when we employed both kidney and heart libraries in parallel for screening interacting partners of α-ENaCC, FLNAC came out as one of the interacting partners from the heart library but not the kidney library. The exact reasons for this outcome remain to be determined, but it may be due in part to the low reproducibility nature of this screen method. Nevertheless, it is important to note that filamin is widely distributed and that we confirmed its interaction with ENaC by one-to-one

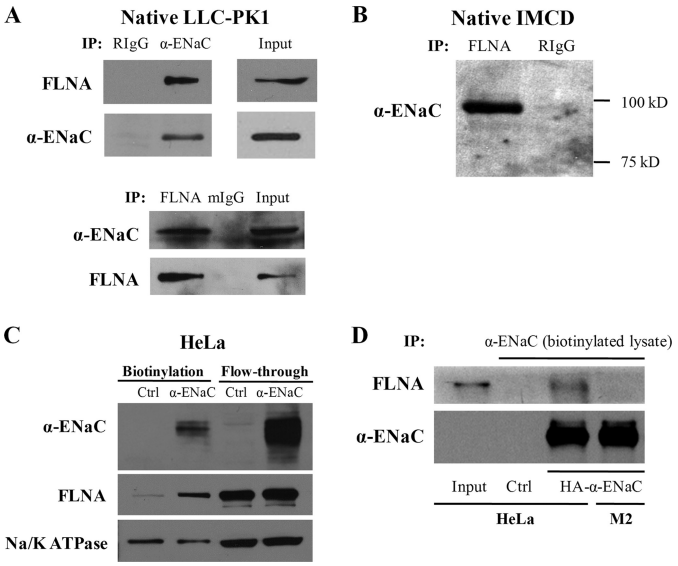

FIGURE 3. **Interaction between endogenous ENaC and filamin A by co-IP.** Data shown here are representative of those from three to four independent experiments. *A,* LLC-PK1 cell lysates were used for reciprocal co-IP using anti-α-ENaC (Calbiochem) and anti-FLNA E-3 for IP and IB as indicated. Nonimmune serum rabbit IgG (*RIgG*) and mouse IgG (*mIgG*) were used as controls. *B*, cell lysates from IMCD cells were precipitated with anti-FLNA H-300 and *RIgG* as control. Immunoprecipitated proteins were analyzed by WB using anti-α-ENaC antibody (Calbiochem). *C,* biotinylation was performed on HeLa cells transfected with either human α-ENaC or empty pcDNA3.1 plasmid (*Ctrl*). Biotinylated proteins were subjected to SDS-PAGE and detected by antibody against ENaC, FLNA, or Na/K-ATPase (as a control). *D,* biotinylation was performed on HeLa and M2 cells transfected with human α-ENaC or empty pcDNA3.1 plasmid (HeLa only, *Ctrl*). Biotinylated proteins were collected using the monomeric avidin kit (Pierce) and proceeded to co-IP assays with α-ENaC antibody. Precipitated proteins were immunoblotted with FLNA H-300 or α-ENaC antibody.

yeast two-hybrid (Fig. 1*A*), GST pulldown (Fig. 1*B*), and by co-IP in renal and nonrenal cell lines (Figs. 2 and 3).

Modulation of ENaC Channel Function by FLNA in Xenopus Oocytes—We co-injected α-, β-, and γ-ENaC mRNAs into oocytes with a concentration ratio of 2:1:1. The average Na^+ current, equal to the total current in the presence of 100 mM Na^+ minus the one when Na^+ was replaced by the equimolar *N*-methyl-D-glucamine, was 2.7 ± 0.3 μA (n = 30) at −50 mV in oocytes expressing ENaC. This Na^+ current was reversibly inhibited by 10 μM amiloride present in the extracellular solution, with the amiloride-sensitive currents averaging 2.42 ± 0.39 μA (n = 17) (Fig. 4), accounting for 90% of the Na^+ current. Co-expression of FLNAC substantially reduced the Na^+ current as well as the amiloride-sensitive current (Fig. 4). In the presence of FLNAC, the amiloride-sensitive current was 0.47 ± 0.21 μA (n = 15), which represents only 19% of the corresponding currents in the absence of FLNAC. The inhibition effect of FLNBC was similar to that of FLNAC (Fig. 4*B*). FLNA also substantially reduced amiloride-sensitive currents in other membrane potentials ranging from −120 to +80 mV, as revealed by use of a voltage ramp protocol (Fig. 4*C*). Although it was reported that efficient trafficking of ENaC to the surface membrane requires assembly of all three subunits (26), individual ENaC subunits are still capable of trafficking to the surface membrane (27). We thus examined the effect of filamin on α-ENaC channel function. When only α-ENaC was expressed in oocytes, significant amiloride-inhibitable currents were observed, although they were much smaller (Fig. 4*D*) than those in the presence of α, β, and γ subunits (Fig. 4). On average, the amiloride-sensitive currents were 181 ± 5 nA (n = 11). Similarly, the co-expression of FLNAC reduced the currents to 71 ± 6 nA (n = 21) (Fig. 4*D*), a 61% reduction. By using a voltage ramp protocol, we found that FLNAC is able to suppress the α-ENaC activity in the tested voltage range of −120 to +80 mV (Fig. 4*E*).

Modulation of ENaC Expression and Distribution by FLNA—To determine whether the reduced whole-cell channel function of ENaC by filamins is due to reduced ENaC expression and surface membrane targeting or reduced single channel activity, we performed WB and biotinylation assays to examine the effect of filamins on the total and plasma membrane expression of α-ENaC, as assessed by densitometry. FLNAC modestly reduced α-ENaC total expression (Fig. 5*A*) as assessed by WB but had no significant effect on its plasma membrane targeting assessed by biotinylation (Fig. 5*B*). By averaging data from three independent experiments, the α-ENaC total expression was reduced to 83 ± 6% by FLNAC (p = 0.005, by paired t test). Furthermore, we performed immunohistochemistry (IHC) experiments to illustrate the effect of filamin on the subcellular distribution of α-ENaC on oocytes that were first tested for amiloride-inhibited currents. We found that, in the presence of FLNAC, the α-ENaC plasma membrane density assessed by IHC in average only reduced to 78% (Fig. 5*C*), which is similar to the reduction in the total ENaC expression. We next calculated the ratio of the α-ENaC amiloride-sensitive current to the plasma membrane density for each tested individual oocyte as a normalized current to assess the channel activity of each α-ENaC protein. We found that in the presence of FLNAC, α-ENaC activity dropped to 52% (n = 4 for each group, p = 0.01, by unpaired t test) (Fig. 5*D*). Taken together, our data from using oocytes indicate that filamin inhibits α-ENaC channel activity, in addition to modestly reducing its overall expression.

We also employed filamin-deficient M2 cells and FLNA-replete A7 cells stably expressing α-ENaC to examine the effect of FLNA on the α-ENaC expression. Our WB analysis revealed that the expression of α-ENaC is reduced with FLNAC co-transfection in M2 cells and is lower in A7 than in M2 cells (Fig. 5*E*), possibly because filamin down-regulates the ENaC expression. Interestingly, endogenous FLNA in A7 cells was significantly reduced by the expression of FLNAC (Fig. 5*E*), suggesting a competitive expression between FLNAC and full-length FLNA. Because the process of selection of stably expressing M2 and A7 cells may have picked up this A7 cell line with lower ENaC expression than the M2 cell line, we next performed transient transfection of α-ENaC to eliminate this potential factor. Furthermore, to avoid/reduce the potential influence of limited protein synthesis capability of cells on the simultaneous expression of two exogenous proteins, we performed transient transfection with α-ENaC plasmid in M2 cells on day 1, followed by an equal split into two wells on day 2 for transient transfection with an empty or FLNAC plasmid. We found that FLNAC significantly reduces the expression of α-ENaC (Fig. 5*F*), in agreement with the results obtained using stable M2 cells (Fig. 5*E*). Averaging from three independent experiments found a reduction to 74 ± 8% (p = 0.003, by paired

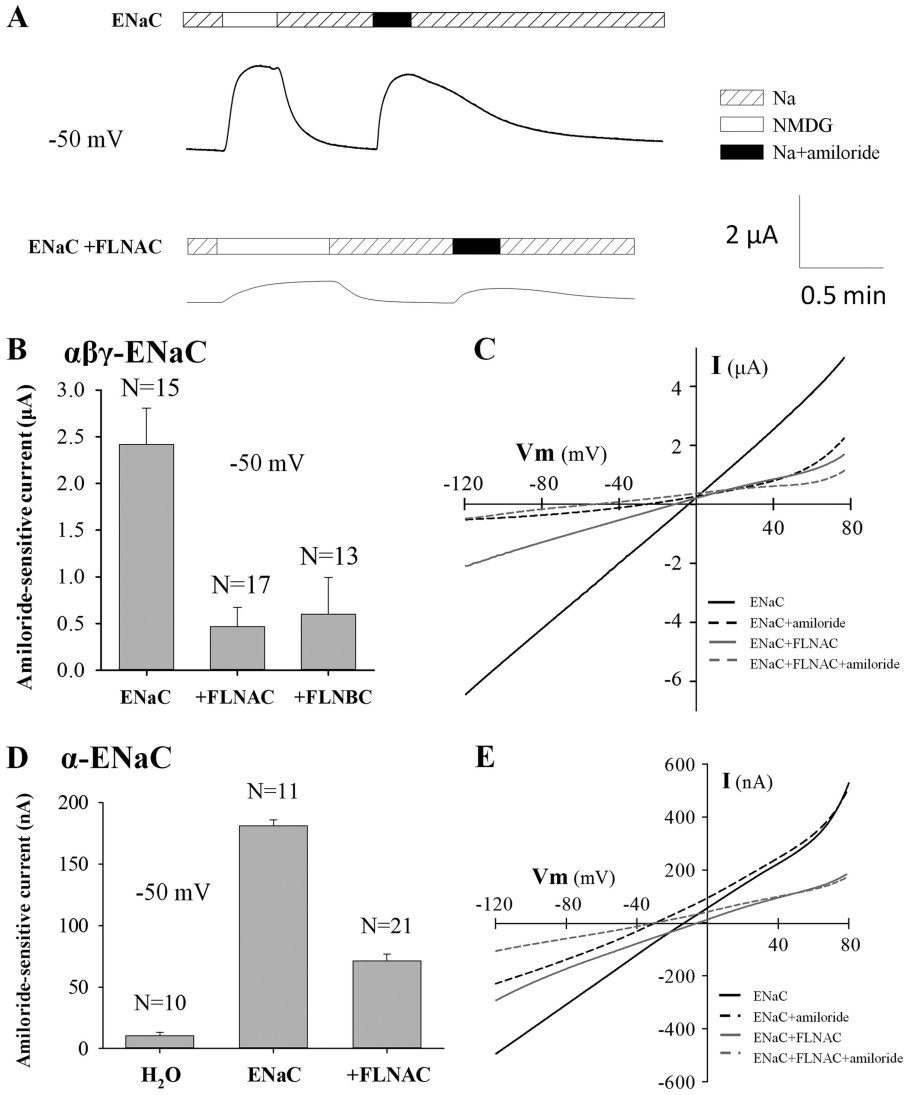

FIGURE 4. **Effect of filamin on whole-cell transport mediated by $\alpha\beta\gamma$-ENaC or α-ENaC overexpressed in *Xenopus* oocytes.** *A,* representative ENaC-mediated whole-cell currents recorded at −50 mV with the two-microelectrode voltage clamp in the presence of the standard Na^+- or NMDG-containing solution, ± amiloride (10 μM), as indicated in an oocyte injected with $\alpha\beta\gamma$-ENaC mRNA together with (*lower panel*) or without (*upper panel*) FLNAC mRNA. *B,* averaged amiloride-sensitive Na^+ currents measured at −50 mV, from oocytes expressing $\alpha\beta\gamma$-ENaC, $\alpha\beta\gamma$-ENaC + FLNAC, or $\alpha\beta\gamma$-ENaC + FLNBC. *C,* representative current-voltage (*I-V*) relationships obtained using a voltage ramp protocol with other conditions similar to *A* and *B*. *D,* effect of FLNAC on α-ENaC function, assessed by amiloride-sensitive Na^+ currents. Shown are averages obtained from using oocytes expressing α-ENaC or α-ENaC + FLNAC ($p <$ 0.001, between ± FLNAC, by unpaired *t* test), or water-injected oocytes. *E,* representative *I-V* curves obtained using a voltage ramp protocol with other conditions similar to *C*.

t test). These data using mammalian melanoma M2 and A7 cells are in agreement with our results obtained using *Xenopus* oocytes that filamin modestly reduces the ENaC expression.

Taken together, we found that there is a modest reduction in the ENaC total (by WB) and plasma membrane (by IHC) expression, which is insufficient to account for the substantial decrease in the whole-cell current in the presence of filamin (Fig. 4). Normalizing the amiloride-sensitive current by the surface membrane density, we found that ENaC channel activity drops to half in the presence of filamin A.

Modulation of α-ENaC Channel Function by FLNAC in Planar Lipid Bilayer—Our data obtained from using *Xenopus* oocytes indicated that FLNA inhibits ENaC single channel activity, in addition to modestly reducing its expression. To verify the inhibition of channel activity, we utilized planar lipid bilayer electrophysiology in combination with tandem affinity purification to purify full-length α-ENaC proteins from the MDCK stable cell line and with *E. coli* purification of FLNAC. We have previously modified and improved the vector construct and affinity purification protocol for use with TRPP2 and TRPP3 channels (25). Indeed, purified α, β, and γ subunits were detectable by Coomassie Blue staining and WB (Fig. 6*A*). After α-ENaC was reconstituted into lipid membrane, single channel openings were observed and showed single channel conductance value compatible with the activities of α-ENaC channels (Fig. 6*B*). In fact, in the presence of 150 mM *cis*-NaCl, single channel conductance was in the 18–21 picosiemens range, larger than when all α, β, and γ subunits are co-expressed, which is consistent with previous reports (28, 29). We then introduced purified FLNAC proteins into the *cis* chamber of the lipid bilayer system to examine whether/how FLNAC affects ENaC single channel activity. We found that addition of

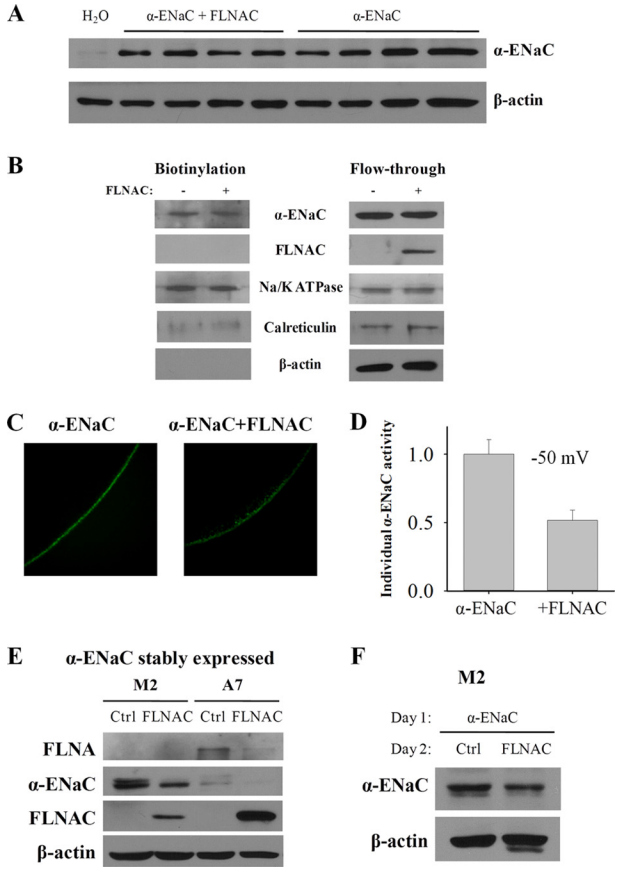

FIGURE 5. **Effect of FLNAC on expression and subcellular distribution of α-ENaC.** *A,* effect of FLNAC on the total expression of α-ENaC. Representative data showing expression of α-ENaC in each individual oocyte assessed by WB. *B,* representative data of three independent experiments showing the effect of FLNAC on the plasma membrane expression of α-ENaC by biotinylation assay. Expressions of Na/K-ATPase, calreticulin, and β-actin serve as controls. *C,* representative IHC data, using anti-α-ENaC antibody PA1–920A, showing the staining of α-ENaC with or without FLNAC co-expression. *D,* effect of FLNAC on the oocyte amiloride-sensitive currents (at −50 mV) normalized by the surface membrane density of α-ENaC assessed by IHC. Shown data are each averaged from four oocytes individually tested for amiloride-sensitive currents and IHC. *E* and *F,* regulation of α-ENaC expression by FLNAC in M2 and A7 cells. *E,* M2 and A7 cells stably expressing α-ENaC were transfected with FLNAC for 48 h. WB was performed to check the expression level with anti-FLNA E-3, anti-α-ENaC 324870, anti-FLNA H-300, and β-actin C-4 for normalization. *F,* M2 cells were transiently transfected with α-ENaC, following by transfection the next day with FLNAC or an empty vector pcDNA3.1 (negative control (*Ctrl*)). Cell lysates were collected after 48 h. α-ENaC expression was detected by WB using anti-α-ENaC 324870 antibody and controlled by β-actin C-4.

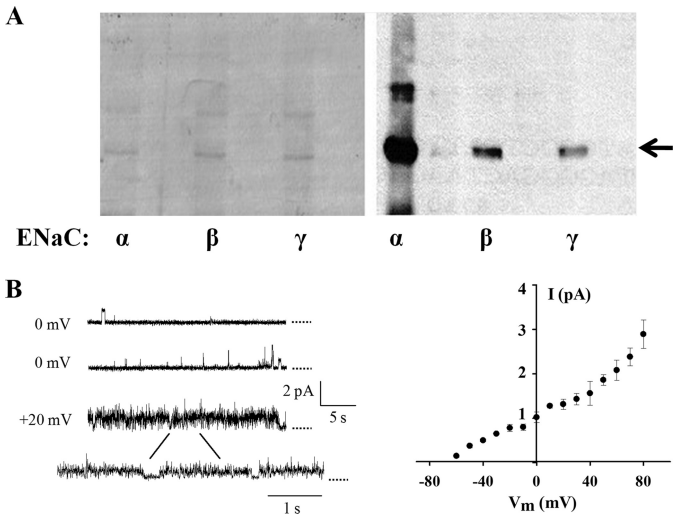

FIGURE 6. **Tandem affinity purification of human α-, β-, and γ-ENaC from MDCK stable cell lines and channel function of α-ENaC reconstituted in lipid bilayer.** *A,* purified human α-, β-, and γ-ENaC channel proteins visualized by Coomassie Blue staining (*left panel*) and WB (*right panel*), as indicated by the *arrow*. All proteins were purified from MDCK cell lines stably transfected with α-, β-, and γ-ENaC cDNAs in the pGTAP3F vector. Antibodies against α-, β-, and γ-ENaC (Santa Cruz Biotechnology) were used for WB. *B,* representative tracings obtained using purified α-ENaC channels reconstituted in the lipid bilayer system (*left panel*) and current-voltage relationship (*right panel*). Single channel activities were recorded under an asymmetrical condition (150/15 mM NaCl on *cis/trans, i.e.* intra/extracellular, compartments). *Dotted lines* indicate closed states.

FLNAC, but not addition of control solution containing denatured (boiled for 5–10 min) FLNAC, substantially inhibits the open probability (NP_o) and mean current, but not the mean open time, of α-ENaC channels (Fig. 7). The corresponding NP_o and mean current values at +40 mV decreased from 2.0 ± 0.4 to 0.5 ± 0.2 ($n = 4$, $p = 0.005$, by paired t test) and from 4.1 ± 1.2 to 1.1 ± 0.4 pA ($n = 4$, $p = 0.01$), respectively (Fig. 7*C*). These experiments demonstrate that FLNAC suppresses ENaC single channel activities, presumably through direct binding. Of note, based on our immunofluorescence experiments (Fig. 5*C*), co-expression of FLNA modestly decreased the plasma membrane expression of ENaC (to 78%), presumably through regulating the half-life of ENaC on the plasma membrane. In contrast, because artificial lipid bilayer has no intracellular systems and FLNA proteins were present during experiments only for some minutes, we can presume that FLNA reduces the P_o value and has no effect on the number of ENaC channels (N) on the bilayer.

DISCUSSION

In this study, we firmly characterized the physical interaction between ENaC and filamin by various *in vitro* and *in vivo* protein-protein binding approaches. Yeast two-hybrid and *E. coli* GST pulldown assays showed interaction between soluble parts of an ENaC subunit and a filamin isoform, presumably through direct binding. In comparison, mammalian cells are more *in vivo* models, and co-IP assays allowed us to show that two full-length proteins interact with each other, although this technique does not tell whether they bind each other directly. Also, when a partner protein is overexpressed, the exhibited interaction may be nonspecific or of an artifactual nature. It was thus important to verify the interaction using native mammalian cells. The fact that the two proteins are in the same complex *in vivo* leads to the question as to what is the functional role of the physical interaction.

Using *Xenopus* oocyte expression model for IHC assays, we showed that the presence of filamin C terminus modestly reduces the surface membrane targeting of α-ENaC. Because similar reductions in the ENaC total expression and surface membrane targeting are insufficient to account for substantially reduced ENaC currents, we concluded that filamin reduces the activity of each individual ENaC channel complex located on the plasma membrane. This was in fact directly demonstrated when comparing normalized amiloride-sensitive currents in the presence and absence of filamin A co-expression

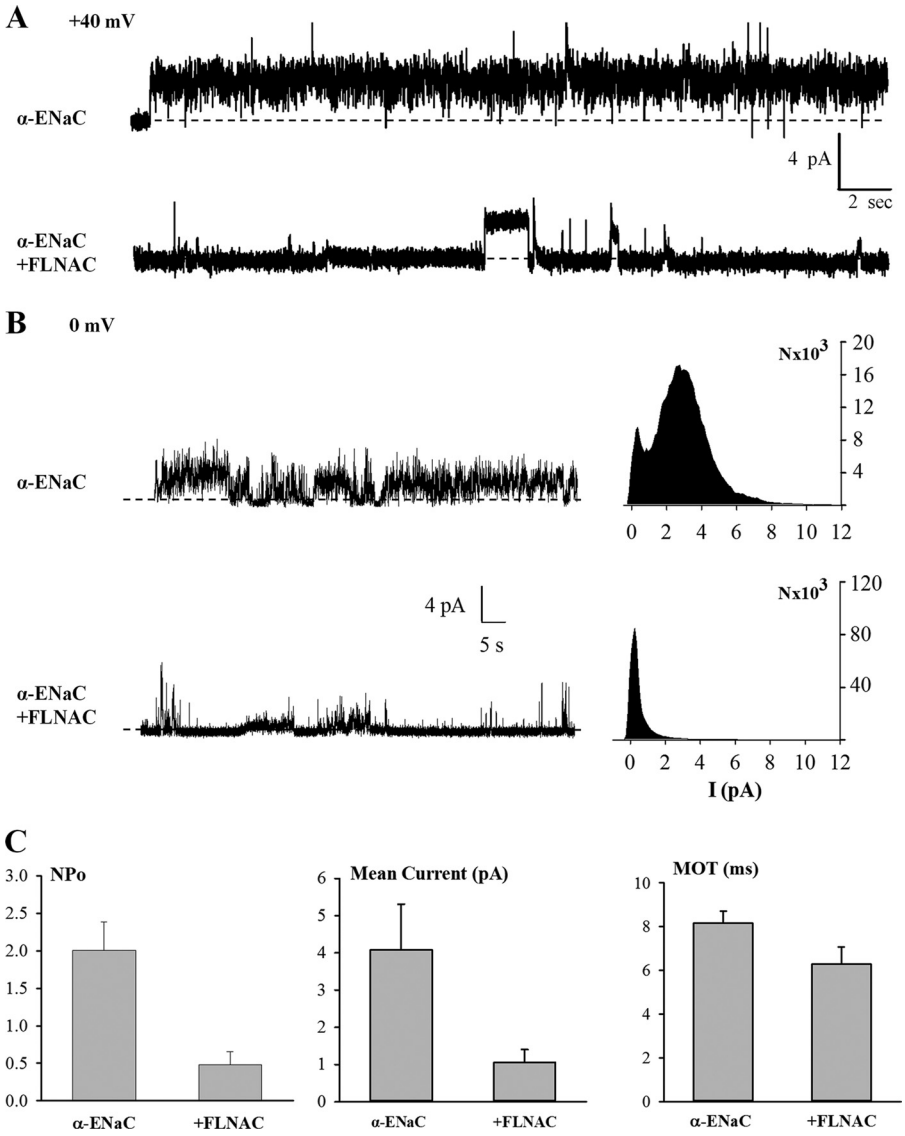

FIGURE 7. **Regulation of α-ENaC channels by FLNAC in a lipid bilayer system.** *A,* representative tracings of reconstituted α-ENaC at +40 mV before and after adding FLNAC to the *cis* chamber. *cis* chamber, 150 mM NaCl; *trans* chamber, 15 mM NaCl. *B,* representative tracings recorded at +0 mV before and after adding FLNAC to the *cis* chamber, and density plots. *Dashed lines* in *A* and *B* indicate closed states. *C,* open probability (NP_o) was calculated and averaged from different patches recorded at +40 mV in the absence (four patches) and presence (four patches) of FLNAC ($p = 0.005$, by paired *t* test). Mean current and mean open time (*MOT*) were also calculated from the same patches and similarly compared ($p = 0.01$ and 0.07, respectively).

(Fig. 5*D*). Of note, it is still possible that the inhibition of ENaC by filamin is indirect, *e.g.* by an intermediate protein. In a recent study, we utilized blocking peptides to disrupt the physical binding between the TRPP3 channel and the RACK1 protein, which abolished the inhibitory effect of RACK1 on TRPP3, demonstrating that the inhibition is mediated by direct physical binding (23). In this study, we performed lipid bilayer experiments using purified ENaC and filamin C terminus for several purposes. First, it confirmed the inhibitory effect of filamin observed in oocytes. Second, it showed that channel inhibition is through direct binding between filamin and α-ENaC. Third, it allowed characterizing ENaC single channel parameters, including NP_o, single channel conductance, and mean open time. In particular, we found that NP_o but not single channel conductance is inhibited by filamin, indicating that filamin gates channel opening through binding to a site in ENaC outside the channel pore.

Given that ENaC is highly selective to Na^+ and the specific effect of amiloride blockade in oocytes, the predicted reversal potential for an amiloride-sensitive I-V curve should be about 70 mV in the presence of 100 mM extracellular Na^+, assuming 6.2 or 6.6 mM intracellular Na^+ (30, 31). However, our observed reversal potential averaged 1.0 ± 0.6 mV ($n = 6$) and 7.1 ± 4.5 mV ($n = 3$) in the absence and presence of FLNAC, respectively (also see Fig. 4*C*). Our results are in agreement with previously reported shift in the reversal potential or resting potential (30, 31). This should be due, at least in part, to loading of Na^+ through overexpressed ENaC channels during incubation for which Na/K-ATPases are unable to counterbalance. Indeed, we observed that oocytes expressing αβγ-ENaC have depolarized resting membrane potentials averaging −2.1 ± 1.3 mV ($n = 6$). This indicates that Na^+ permeability (via ENaC), in addition to K^+ and Cl^- permeabilities (via native K^+ and Cl^- channels), plays an important role in defining the oocyte resting potential

and results in significant intracellular Na^+ accumulation. Of note, intracellular concentrations of K^+ and Cl^-, in addition to that of Na^+, also significantly changed in oocytes overexpressing ENaC (31), indicating that K^+ and Cl^- permeabilities remain important for the resting potential. The resting potential became more negative and oocytes appeared healthier when 2 μM amiloride was added to the incubation medium, FLNAC was co-expressed (-10.2 ± 1.6 mV, $n = 3$), and/or only the α subunit was expressed, presumably because intracellular Na^+ concentration was much lower than extracellular Na^+ concentration under these conditions, as a consequence of much reduced Na^+ loading via ENaC. Consistently, under these conditions, the reversal potential for the amiloride-sensitive I-V became more positive (7.1 mV, with FLNA co-expression; also see *e.g.* Fig. 4, *C* and *E*).

The mammalian cytoskeleton is composed of three major protein families as follows: microfilaments, microtubules, and intermediate filaments, as well as numerous cytoskeleton-associated proteins (32). They are implicated in cell shape, motility, signal transduction, vesicular trafficking, and function of ion channel/transporter/receptor. The actin-based cytoskeleton has been shown to interact indirectly and directly with ion channels and membrane transport proteins (33–35). The hypothesis that actin cytoskeleton is directly involved in regulation of ENaC was first supported by a immunocolocalization study showing ENaC channels always present in close proximity to actin filaments and further demonstrated by characterizing the modulatory role of actin filament organization on ENaC channel activity in A6 epithelial cells (18). In this study, Cantiello *et al.* (18) also revealed a potential functional regulation of ENaC by full-length filamin protein in A6 cells. However, whether there is physical interaction between ENaC and filamin, which domains are involved in the interaction, and whether the functional regulation is through the physical interaction remained unclear. This study specifically answered these questions by using various *in vitro* and *in vivo* protein-protein interaction approaches and by electrophysiological analyses.

It was reported that dimerization of filamin is mediated by a C-terminal domain and that the majority of filamin interacting partners bind its C terminus as well (36). Filamin N terminus binds actin thereby cross-linking cortical actin into a dynamic three-dimensional structure. Our data suggest that the binding of FLNAC to ENaC C terminus is enough to inhibit the channel function. Thus, it is possible that the filamin N terminus serves to stabilize ENaC via cross-linking with the actin network. Future studies would examine whether and how the filamin-ENaC interaction is critical to the physiological functions currently known to be associated with ENaC or filamins.

Acknowledgment—We are grateful for the valuable discussions with and comments by Horacio Cantiello.

REFERENCES

1. Canessa, C. M., Schild, L., Buell, G., Thorens, B., Gautschi, I., Horisberger, J. D., and Rossier, B. C. (1994) Amiloride-sensitive epithelial Na^+ channel is made of three homologous subunits. *Nature* **367,** 463–467
2. Barbry, P., and Hofman, P. (1997) Molecular biology of Na^+ absorption. *Am. J. Physiol.* **273,** G571–G585
3. Kellenberger, S., and Schild, L. (2002) Epithelial sodium channel/degenerin family of ion channels. A variety of functions for a shared structure. *Physiol. Rev.* **82,** 735–767
4. Mano, I., and Driscoll, M. (1999) DEG/ENaC channels. A touchy superfamily that watches its salt. *BioEssays* **21,** 568–578
5. Lingueglia, E., Deval, E., and Lazdunski, M. (2006) FMRF-amide-gated sodium channel and ASIC channels. A new class of ionotropic receptors for FMRF-amide and related peptides. *Peptides* **27,** 1138–1152
6. Zuckerman, J. B., Chen, X., Jacobs, J. D., Hu, B., Kleyman, T. R., and Smith, P. R. (1999) Association of the epithelial sodium channel with Apx and α-spectrin in A6 renal epithelial cells. *J. Biol. Chem.* **274,** 23286–23295
7. Mazzochi, C., Bubien, J. K., Smith, P. R., and Benos, D. J. (2006) The carboxyl terminus of the α-subunit of the amiloride-sensitive epithelial sodium channel binds to F-actin. *J. Biol. Chem.* **281,** 6528–6538
8. Awayda, M. S., and Subramanyam, M. (1998) Regulation of the epithelial Na^+ channel by membrane tension. *J. Gen. Physiol.* **112,** 97–111
9. Satlin, L. M., Sheng, S., Woda, C. B., and Kleyman, T. R. (2001) Epithelial Na^+ channels are regulated by flow. *Am. J. Physiol. Renal Physiol.* **280,** F1010–F1018
10. Rossier, B. C., Pradervand, S., Schild, L., and Hummler, E. (2002) Epithelial sodium channel and the control of sodium balance. Interaction between genetic and environmental factors. *Annu. Rev. Physiol.* **64,** 877–897
11. Schild, L. (2004) The epithelial sodium channel: from molecule to disease. *Rev. Physiol. Biochem. Pharmacol.* **151,** 93–107
12. Gormley, K., Dong, Y., and Sagnella, G. A. (2003) Regulation of the epithelial sodium channel by accessory proteins. *Biochem. J.* **371,** 1–14
13. Feng, Y., and Walsh, C. A. (2004) The many faces of filamin. A versatile molecular scaffold for cell motility and signalling. *Nat. Cell Biol.* **6,** 1034–1038
14. van der Flier, A., and Sonnenberg, A. (2001) Structural and functional aspects of filamins. *Biochim. Biophys. Acta* **1538,** 99–117
15. Stossel, T. P., Condeelis, J., Cooley, L., Hartwig, J. H., Noegel, A., Schleicher, M., and Shapiro, S. S. (2001) Filamins as integrators of cell mechanics and signalling. *Nat. Rev. Mol. Cell Biol.* **2,** 138–145
16. Takafuta, T., Saeki, M., Fujimoto, T. T., Fujimura, K., and Shapiro, S. S. (2003) A new member of the LIM protein family binds to filamin B and localizes at stress fibers. *J. Biol. Chem.* **278,** 12175–12181
17. Cantiello, H. F., Prat, A. G., Bonventre, J. V., Cunningham, C. C., Hartwig, J. H., and Ausiello, D. A. (1993) Actin-binding protein contributes to cell volume regulatory ion channel activation in melanoma cells. *J. Biol. Chem.* **268,** 4596–4599
18. Cantiello, H. F., Stow, J. L., Prat, A. G., and Ausiello, D. A. (1991) Actin filaments regulate epithelial Na^+ channel activity. *Am. J. Physiol.* **261,** C882–C888
19. Thelin, W. R., Chen, Y., Gentzsch, M., Kreda, S. M., Sallee, J. L., Scarlett, C. O., Borchers, C. H., Jacobson, K., Stutts, M. J., and Milgram, S. L. (2007) Direct interaction with filamins modulates the stability and plasma membrane expression of CFTR. *J. Clin. Invest.* **117,** 364–374
20. Wang, Q., Dai, X.-Q., Li, Q., Wang, Z., Cantero Mdel, R., Li, S., Shen, J., Tu, J.-C., Cantiello, H., and Chen, X. Z. (2012) Structural interaction and functional regulation of polycystin-2 by filamin. *PLoS ONE* **7,** e40448
21. Jovov, B., Tousson, A., Ji, H. L., Keeton, D., Shlyonsky, V., Ripoll, P. J., Fuller, C. M., and Benos, D. J. (1999) Regulation of epithelial Na^+ channels by actin in planar lipid bilayers and in the *Xenopus* oocyte expression system. *J. Biol. Chem.* **274,** 37845–37854
22. Li, Q., Montalbetti, N., Shen, P. Y., Dai, X. Q., Cheeseman, C. I., Karpinski, E., Wu, G., Cantiello, H. F., and Chen, X. Z. (2005) α-Actinin associates with polycystin-2 and regulates its channel activity. *Hum. Mol. Genet.* **14,** 1587–1603
23. Yang, J., Wang, Q., Zheng, W., Tuli, J., Li, Q., Wu, Y., Hussein, S., Dai, X. Q., Shafiei, S., Li, X. G., Shen, P. Y., Tu, J. C., and Chen, X. Z. (2012) Receptor for activated C kinase 1 (RACK1) inhibits function of transient receptor potential (TRP)-type channel Pkd2L1 through physical interaction. *J. Biol. Chem.* **287,** 6551–6561
24. Chen, X. Z., Vassilev, P. M., Basora, N., Peng, J. B., Nomura, H., Segal, Y., Brown, E. M., Reeders, S. T., Hediger, M. A., and Zhou, J. (1999) Polycystin-L is a calcium-regulated cation channel permeable to calcium ions. *Nature* **401,** 383–386

25. Li, Q., Dai, X. Q., Shen, P. Y., Cantiello, H. F., Karpinski, E., and Chen, X. Z. (2004) A modified mammalian tandem affinity purification procedure to prepare functional polycystin-2 channel. *FEBS Lett.* **576,** 231–236
26. Snyder, P. M. (2005) Regulation of epithelial Na^+ channel trafficking. *Endocrinology* **146,** 5079–5085
27. Weisz, O. A., Wang, J. M., Edinger, R. S., and Johnson, J. P. (2000) Non-coordinate regulation of endogenous epithelial sodium channel (ENaC) subunit expression at the apical membrane of A6 cells in response to various transporting conditions. *J. Biol. Chem.* **275,** 39886–39893
28. Kizer, N., Guo, X. L., and Hruska, K. (1997) Reconstitution of stretch-activated cation channels by expression of the α-subunit of the epithelial sodium channel cloned from osteoblasts. *Proc. Natl. Acad. Sci. U.S.A.* **94,** 1013–1018
29. Ismailov, I. I., Awayda, M. S., Berdiev, B. K., Bubien, J. K., Lucas, J. E., Fuller, C. M., and Benos, D. J. (1996) Triple-barrel organization of ENaC, a cloned epithelial Na^+ channel. *J. Biol. Chem.* **271,** 807–816
30. McDonald, F. J., Snyder, P. M., McCray, P. B., Jr., and Welsh, M. J. (1994) Cloning, expression, and tissue distribution of a human amiloride-sensitive Na^+ channel. *Am. J. Physiol.* **266,** L728–L734
31. Nakhoul, N. L., Hering-Smith, K. S., Abdulnour-Nakhoul, S. M., and Hamm, L. L. (2001) Ammonium interaction with the epithelial sodium channel. *Am. J. Physiol. Renal Physiol.* **281,** F493–F502
32. Khurana, S. (2000) Role of actin cytoskeleton in regulation of ion transport. Examples from epithelial cells. *J. Membr. Biol.* **178,** 73–87
33. Noda, Y., Horikawa, S., Katayama, Y., and Sasaki, S. (2004) Water channel aquaporin-2 directly binds to actin. *Biochem. Biophys. Res. Commun.* **322,** 740–745
34. Chasan, B., Geisse, N. A., Pedatella, K., Wooster, D. G., Teintze, M., Carattino, M. D., Goldmann, W. H., and Cantiello, H. F. (2002) Evidence for direct interaction between actin and the cystic fibrosis transmembrane conductance regulator. *Eur. Biophys. J.* **30,** 617–624
35. Cantiello, H. F. (1997) Role of actin filament organization in cell volume and ion channel regulation. *J. Exp. Zool.* **279,** 425–435
36. Zhou, A. X., Hartwig, J. H., and Akyürek, L. M. (2010) Filamins in cell signaling, transcription, and organ development. *Trends Cell Biol.* **20,** 113–123